Ordered Aerogels

DOI: 10.1002/ange.201405123

Aerogels with 3D Ordered Nanofiber Skeletons of Liquid-Crystalline Nanocellulose Derivatives as Tough and Transparent Insulators**

Yuri Kobayashi, Tsuguyuki Saito, and Akira Isogai*

Abstract: *Aerogels of high porosity and with a large internal surface area exhibit outstanding performances as thermal, acoustic, or electrical insulators. However, most aerogels are mechanically brittle and optically opaque, and the structural and physical properties of aerogels strongly depend on their densities. The unfavorable characteristics of aerogels are intrinsic to their skeletal structures consisting of randomly interconnected spherical nanoparticles. A structurally new type of aerogel with a three-dimensionally ordered nanofiber skeleton of liquid-crystalline nanocellulose (LC-NCell) is now reported. This LC-NCell material is composed of mechanically strong, surface-carboxylated cellulose nanofibers dispersed in a nematic LC order. The LC-NCell aerogels are transparent and combine mechanical toughness and good insulation properties. These properties of the LC-NCell aerogels could also be readily controlled.*

Aerogels are low-density solids with high porosity and a large internal surface area.[1–3] Representative examples include silica, resorcinol/formaldehyde (RF), and carbon aerogels. These aerogels have in common a network skeleton of randomly interconnected spherical nanoparticles, which define a system of well-accessible pores.[4] Porous materials with such structural properties demonstrate outstanding performances as thermal, acoustic, or electrical insulators, catalyst supports, drug carriers, cosmic dust collectors, and nuclear waste storage materials.[2–4] However, two issues that need to be addressed for the practical use of aerogels still remain: 1) their mechanical brittleness and 2) the energy- and time-consuming fabrication process, which requires temperature control, solvent exchange, and supercritical drying. In particular, the mechanical brittleness of aerogels is intrinsic to their skeletal structure and limits their applications. Whereas the hybridization of aerogels with organic polymers is a promising approach for reinforcement,[5,6] it also induces significant decreases in porosity and surface area.

Nanocellulose, or nanofibrillated native cellulose,[7] has recently been attracting interest as a building block for aerogels.[8–14] Cellulose is produced in plant tissues in the form of crystalline nanofibers with a width of approximately 3 nm. These nanofibers have a low density (1.6 $g\,cm^{-3}$), a high strength (2–3 GPa), a high elastic modulus (110–140 GPa), and a large surface area (ca. 800 $m^2\,g^{-1}$); all of these properties render these nanofibers very suitable for aerogel skeletons.[15–17] Nanocellulose aerogels are thus mechanically tough and flexible.[11] However, unlike silica aerogels,[4] these aerogels show no optical transparency and no linear elasticity and have much lower surface areas than expected. These unfavorable properties of the nanocellulose aerogels are related to their skeletal structures, which consist of randomly connected bundled nanofibers. Foam structures of nanocellulose and aerogels of regenerated cellulose prepared through molecular dissolution processes have also been described.[18–22]

Herein, we report a structurally new type of aerogel that combines good heat insulation, optical transparency, and mechanical toughness. These aerogels consist of three-dimensionally ordered nanofiber skeletons of liquid-crystalline nanocellulose (LC-NCell; Figure 1). The LC-NCell used in the present study is composed of surface-carboxylated cellulose nanofibers dispersed in water in a nematic LC order and was prepared from wood cellulose by an oxidation reaction using 2,2,6,6-tetramethylpiperidine-1-oxyl (TEMPO) as the catalyst.[23–25] The liquid-crystalline arrange-

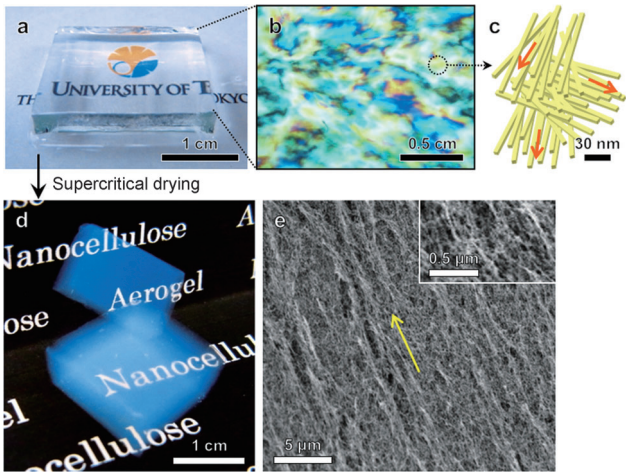

Figure 1. Transparent aerogels with 3D ordered LC-NCell nanofiber skeletons. a) LC-NCell hydrogel (1% w/v). b) Birefringence image of the hydrogel. c) A simplified model of the liquid-crystalline arrangement of the nanofibers or the nematic multi-domain structure. d) LC-NCell aerogels obtained by supercritical drying of the hydrogels. e) SEM images of a cross-section of the aerogel, showing a domain of the oriented nanofibers.

[*] Y. Kobayashi, Assoc. Prof. T. Saito, Prof. A. Isogai
Department of Biomaterials Science, The University of Tokyo
1-1-1 Yayoi, Bunkyo-ku, Tokyo (Japan)
E-mail: asaitot@mail.ecc.u-tokyo.ac.jp

[**] This study was partially supported by Grants-in-Aids for Scientific Research (23688020 and 21228007) from the Japan Society for the Promotion of Science (JSPS) and by the Core Research for Evolutional Science and Technology (CREST) program of the Japan Science and Technology Agency (JST).

Supporting information for this article is available on the WWW under http://dx.doi.org/10.1002/anie.201405123.

ment of the nanofibers could be fixed using a dilute acid solution,[25] so that the fluid LC-NCell dispersions became stiff free-standing hydrogels without volume shrinkage (Figure 1 a–c). Transparent LC-NCell aerogels were obtained by supercritical drying of these hydrogels (Figure 1 d; see the Supporting Information for experimental details). The ordered nanofiber network of the hydrogels was preserved in the aerogels even throughout the drying process (Figure 1 e; see also the Supporting Information, Figure S1).

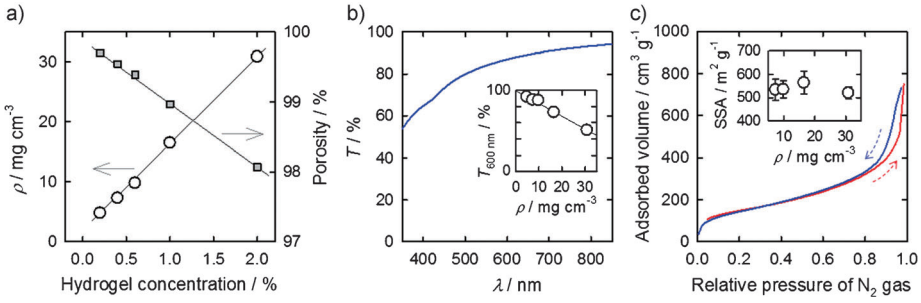

Figure 2. Structural characteristics of LC-NCell aerogels. a) Density and porosity of the aerogel as a function of hydrogel concentration. b) Light transmittance spectrum of the 1 mm thick aerogel with a density of 10 mg cm^{-3}. Inset: light transmittance at 600 nm as a function of density. c) Nitrogen adsorption–desorption isotherm of the aerogel. Inset: SSA of the aerogels estimated from the isotherms.

The structural properties of the LC-NCell aerogels can be easily regulated (Figure 2). The bulk densities (ρ) of the aerogels were found to increase in a linear manner with hydrogel concentration (Figure 2 a). The LC-NCell aerogels prepared in the present study had very low densities (4 to 40 mg cm^{-3}; porosity: 98.1–99.7 %), and are thus categorized into the lowest density class of lightweight porous materials. A low aerogel density results in a smaller dielectric constant and lower thermal conductivity.[2,4] Upon drying of the hydrogels, the LC-NCell aerogels exhibited linear shrinkages of approximately 14 %. These shrinkages were uniform for each side of the cube-shaped aerogels, suggesting that the LC-NCell aerogels were isotropic as bulk structures. In general, a linear shrinkage of 10–15 % is inevitable when supercritical drying is used to prepare aerogels.[4]

Figure 2 b shows the UV/Vis light transmittance spectrum of the LC-NCell aerogel. The 1 mm thick LC-NCell aerogel, with a density of approximately 10 mg cm^{-3}, showed a high transmittance of 80–90 % in the visible-light region, which decreased moderately in a linear manner with density (Figure 2 b, inset). These aerogels did not absorb in the visible-light region; the LC-NCell aerogels are therefore colorless, as are silica aerogels.[4] The blue appearance of the LC-NCell aerogels (Figure 1 d) is caused by Rayleigh scattering of short-wavelength light by their thin skeletons.

The nitrogen adsorption isotherms of the LC-NCell aerogels were characterized by hysteresis at a high relative pressure (Figure 2 c). Such an isotherm is often observed for mesoporous structures with pore sizes of 2–50 nm.[26] The pores of the LC-NCell aerogels correspond to the spaces between the oriented nanofibers (Figure 1 e). The pore size of the LC-NCell aerogels as estimated from the isotherms ranged from a few nanometers to 100 nm, with a most probable value of approximately 30 nm with the increase in density (Figure S2). The specific surface areas (SSAs) of the LC-NCell aerogels were almost constant within a narrow range of 500–600 m^2 g^{-1} (Figure 2 c, inset), indicating that the contact areas between the nanofibers remained constant even as the density was changed. From the SSA values, the nanofiber width of the aerogel skeleton could be estimated to be 4–5 nm, which is close to the width of isolated cellulose nanofibers (ca. 3 nm). A large SSA is important for the application of aerogels as insulators, supports, and adsorbents.[3,7,27]

A significant advantage of LC-NCell aerogels over common aerogels, such as silica, RF, and carbon, is their mechanical toughness. Compression stress–strain curves for the LC-NCell aerogels are shown in Figure 3 a. The LC-NCell aerogels showed linear elasticity at low strains of less than 10 %. After a yielding point, a plastic region with a gradual

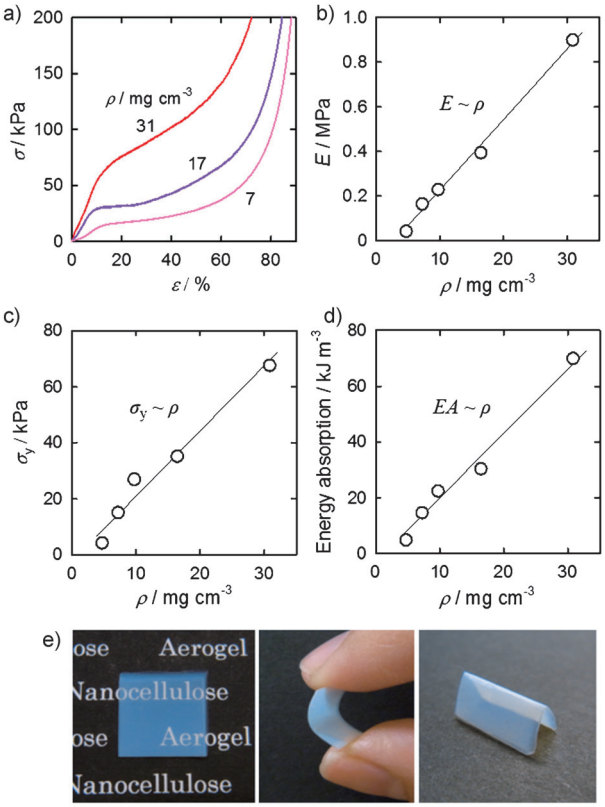

Figure 3. Mechanical properties of the LC-NCell aerogels. a) Compression stress–strain (σ–ε) curves of the aerogels. b) Compression modulus (E), c) yield stress (σ_y), and d) energy absorption of the aerogels calculated from the stress–strain curves. e) Transparency and flexibility of the densified aerogels after compression.

increase in stress in response to a large deformation, or energy absorption, was observed. The plastic deformations of the LC-NCell aerogel skeletons were likely caused by plastic buckling of the nanofibers and/or interfacial slippage at the joint parts between the nanofibers. At high strains of more than 60%, the LC-NCell aerogels showed strong strain hardening, which is due to densification of their skeletons. This type of tough stress–strain behavior on compression is observed for foam structures of cellulose and other synthetic polymers.[19,28] However, these foam materials are optically opaque and have low SSA values of less than 50 $m^2 g^{-1}$. Although some silica aerogels combine optical transparency and large SSA values, such aerogels are mechanically brittle and fracture at low strains. Silica-based organic–inorganic hybrid aerogels that show rubber-like, non-linear elasticity in response to large deformations without energy absorption have recently been reported.[29]

The compression elastic modulus, yield stress, and energy absorption of the LC-NCell aerogels increased in a linear manner with density (Figure 3b–d). The elastic modulus (E) of silica, as well as those of various organic and carbon aerogels, follows the following power law as a function of density:

$$E \sim \rho^{\alpha} \quad (1)$$

with the power α between 2.0 and 3.6.[4] This strong dependence of the modulus on the density is explained by the heterogeneous network structures of the aerogels, which contain more dangling, non-bridging skeletons at low densities. Therefore, it is significant that $\alpha = 1$ for the LC-NCell aerogels at low densities of 4–40 mg cm^{-3}, because it indicates that the skeletons of the LC-NCell aerogels are structurally new, homogeneous, and regulated. No scaling laws for yield stress and energy absorption have been reported for conventional aerogels that fracture at low strains. In fact, the energy absorption of LC-NCell aerogels, which scales with density, is inherently higher than those of these brittle aerogels. It is also noteworthy that the aerogels that were densified by compression were still transparent, flexible, and foldable (Figure 3e) and retained large SSA values of over 500 $m^2 g^{-1}$.

The specific compression moduli, SSA values, and the optical transparency of various aerogels are plotted in Figure 4. The LC-NCell aerogels prepared in the present study were similar to the silica aerogels in terms of the specific compression modulus, SSA, and optical transparency. These properties of the LC-NCell aerogels distinguishes them from RF, carbon, and other cellulose aerogels. Furthermore, considering that the toughness of the LC-NCell aerogels is also superior to those of silica, RF, and carbon aerogels (Figure 3), the present LC-NCell aerogels with a structurally new type of skeleton display unique physical properties.

In addition, the LC-NCell aerogels exhibited very low thermal conductivity (Figure 5). The lowest thermal conductivity of 0.018 $W m^{-1} K^{-1}$ was measured at a density of 17 mg cm^{-3}, and it increased as the density was increased. This value is comparable to the lowest values reported for silica aerogels in air (0.015 $W m^{-1} K^{-1}$) and is lower than those of commercially available insulators, such as polyurethane

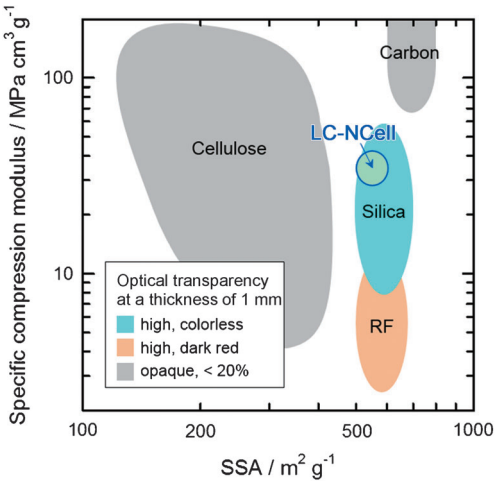

Figure 4. Properties of various aerogels in terms of the specific compression modulus, SSA, and optical transparency. Typical values were plotted for silica ($\rho = 0.1$–0.2 g cm^{-3}), RF ($\rho = 0.04$–0.08 g cm^{-3}), and carbon ($\rho = 0.08$–0.3 g cm^{-3}) aerogels.[2,30–33] The values for cellulose aerogels were adapted from the literature.[11,12,20–22]

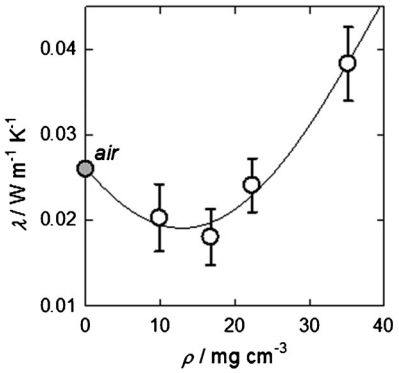

Figure 5. Thermal conductivity (λ) of the LC-NCell aerogel as a function of density.

foam, carbonized cork, and mineral wools (0.03–0.05 $W m^{-1} K^{-1}$).[2,3] In theory, the thermal conductivity of an aerogel in air is approximated by the sum of the heat transfer by the solid phase (skeleton; λ_{solid}), the gas phase (λ_{gas}), and the radiation (λ_{rad}):[4]

$$\lambda_{aerogel} = \lambda_{solid} + \lambda_{gas} + \lambda_{rad} \quad (2)$$

The contributions of the solid phase (λ_{solid}) and the gas phase (λ_{gas}) can be significantly reduced by lowering the bulk density of the aerogel and by narrowing the pore size to less than the mean free path of gas molecules in air (ca. 70 nm), respectively. The LC-NCell aerogels with the lowest conductivity displayed both a very low density of 17 mg cm^{-3} and a characteristic pore size of approximately 30 nm (Figure S2), which should account for the significant reduction in conductivity of this aerogel to a value that is smaller than the conductivity of air.

In conclusion, a structurally new type of aerogel with a three-dimensionally ordered nanofiber skeleton was prepared from surface-carboxylated LC-NCell dispersions through acid-induced gelation and supercritical drying. The LC-NCell can be produced from native wood cellulose through a water-based process that requires only a low energy input. The resulting LC-NCell aerogels are transparent and combine mechanical toughness and good heat insulation, which is a combination not observed with conventional aerogels. These structural and physical properties of the aerogels are also highly controllable. Therefore, LC-NCell aerogels can be used as a novel high-performance insulator with optical transparency and mechanical toughness.

Received: May 8, 2014
Published online: July 1, 2014

Keywords: aerogels · insulation · liquid crystals · mesoporous materials · nanocellulose

[1] S. Kistler, *Nature* **1931**, *127*, 741.
[2] N. Hüsing, U. Schubert, *Angew. Chem. Int. Ed.* **1998**, *37*, 22; *Angew. Chem.* **1998**, *110*, 22.
[3] A. C. Pierre, G. M. Pajonk, *Chem. Rev.* **2002**, *102*, 4243.
[4] G. Reichenauer, Z. Bayern in *Kirk-Othmer Encyclopedia of Chemical Technology*, Wiley, New York, **2008**.
[5] N. Leventis, *Acc. Chem. Res.* **2007**, *40*, 874.
[6] D. J. Boday, P. Y. Keng, B. Muriithi, J. Pyun, D. A. Loy, *J. Mater. Chem.* **2010**, *20*, 6863.
[7] D. Klemm, F. Kramer, S. Moritz, T. Lindstrom, M. Ankerfors, D. Gray, A. Dorris, *Angew. Chem. Int. Ed.* **2011**, *50*, 5438; *Angew. Chem.* **2011**, *123*, 5550.
[8] R. T. Olsson, M. A. S. A. Samir, G. Salazar-Alvarez, L. Belova, V. Ström, L. A. Berglund, O. Ikkala, J. Nogués, U. W. Gedde, *Nat. Nanotechnol.* **2010**, *5*, 584.
[9] M. Wang, I. V. Anoshkin, A. G. Nasibulin, J. T. Korhonen, J. Seitsonen, J. Pere, E. I. Kauppinen, R. H. A. Ras, O. Ikkala, *Adv. Mater.* **2013**, *25*, 2428.
[10] M. Hamedi, E. Karabulut, A. Marais, A. Herland, G. Nyström, L. Wågberg, *Angew. Chem. Int. Ed.* **2013**, *52*, 12038; *Angew. Chem.* **1998**, *125*, 12260.
[11] M. Pääkkö, J. Vapaavuori, R. Silvennoinen, H. Kosonen, M. Ankerfors, T. Lindström, L. A. Berglund, O. Ikkala, *Soft Matter* **2008**, *4*, 2492.
[12] H. Sehaqui, Q. Zhou, L. A. Berglund, *Compos. Sci. Technol.* **2011**, *71*, 1593.
[13] W. Chen, Q. Li, Y. Wang, X. Yi, J. Zeng, H. Yu, Y. Liu, J. Li, *ChemSusChem* **2014**, *7*, 154.
[14] L. Heath, W. Thielemans, *Green Chem.* **2010**, *12*, 1448.
[15] I. Sakurada, Y. Nukushina, T. Ito, *J. Polym. Sci.* **1962**, *57*, 651.
[16] J. Wohlert, M. Bergenstråhle-Wohlert, L. A. Berglund, *Cellulose* **2012**, *19*, 1821.
[17] T. Saito, R. Kuramae, J. Wohlert, L. A. Berglund, A. Isogai, *Biomacromolecules* **2013**, *14*, 248.
[18] A. J. Svagan, M. A. S. A. Samir, L. A. Berglund, *Adv. Mater.* **2008**, *20*, 1263.
[19] H. Sehaqui, M. Salajková, Q. Zhou, L. A. Berglund, *Soft Matter* **2010**, *6*, 1824.
[20] J. Cai, S. Liu, J. Feng, S. Kimura, M. Wada, S. Kuga, L. Zhang, *Angew. Chem. Int. Ed.* **2012**, *51*, 2076; *Angew. Chem.* **2012**, *124*, 2118.
[21] F. Liebner, E. Haimer, A. Potthast, D. Loidl, S. Tschegg, M. A. Neouze, M. Wendland, T. Rosenau, *Holzforschung* **2009**, *63*, 3.
[22] R. Sescousse, R. Gavillon, T. Budtova, *Carbohydr. Polym.* **2011**, *83*, 1766.
[23] T. Saito, Y. Nishiyama, J.-L. Putaux, M. Vignon, A. Isogai, *Biomacromolecules* **2006**, *7*, 1687.
[24] A. Isogai, T. Saito, H. Fukuzumi, *Nanoscale* **2011**, *3*, 71.
[25] T. Saito, T. Uematsu, S. Kimura, T. Enomae, A. Isogai, *Soft Matter* **2011**, *7*, 8804.
[26] K. S. W. Sing, D. H. Everett, R. A. W. Haul, L. Moscou, R. A. Pierotti, J. Rouquérol, T. Siemieniewska, *Pure Appl. Chem.* **1985**, *57*, 603.
[27] C. Bi, G. H. Tang, *Int. J. Heat Mass Transfer* **2013**, *64*, 452.
[28] L. J. Gibson, M. F. Ashby, *Cellular Solids: Structure and Properties*, Cambridge University Press, Cambridge, UK, **1997**.
[29] K. Kanamori, M. Aizawa, K. Nakanishi, T. Hanada, *Adv. Mater.* **2007**, *19*, 1589.
[30] O. Nikel, A. M. Anderson, M. K. Carroll, W. D. Keat, *J. Non-Cryst. Solids* **2011**, *357*, 3176.
[31] K. E. Parmenter, F. Milstein, *J. Non-Cryst. Solids* **1998**, *223*, 179.
[32] R. W. Pekala, C. T. Alviso, J. D. LeMay, *J. Non-Cryst. Solids* **1990**, *125*, 67.
[33] R. W. Pekala, *J. Mater. Sci.* **1989**, *24*, 3221.

